International Journal of Heat and Technology
Vol. 44, No. 1, February, 2026, pp. 34-44
Journal homepage: http://iieta.org/journals/ijht

An Experimental and Numerical Evaluation of PV Performance Enhancement by Radiative Cooling Using Indium Tin Oxide Nano-Coating

Saddam K. Shabeeb[1*], Hussain H. Al-Kayiem[2], Saad O. Ismael[1], Qasim S. Mahdi[3], Dhamyaa S. Khudhur[1]

[1] Mechanical Engineering Department, College of Engineering, Mustansiriyah University, Baghdad 10001, Iraq
[2] College of Engineering Technology, University of Hilla, Al-Hilla 51001, Iraq
[3] Biomedical Engineering Department, College of Engineering, Ashur University, Baghdad 10064, Iraq

Corresponding Author Email: saddamaltamimi1@gmail.com

https://doi.org/10.18280/ijht.440104

Received: 28 September 2025
Revised: 4 November 2025
Accepted: 13 November 2025
Available online: 28 February 2026

Keywords:
Indium Tin Oxide nano-coating, PV passive cooling, PV nano-coating, PV radiative cooling, solar power generation, transmittance analysis

ABSTRACT

The response range of photovoltaic cells to radiation is between 0.3–1.1 μm, and the bulk of the radiation band outside this range is converted into heat. Hence, any method that reduces the accumulated radiation-to-heat is a considerable enhancement in the performance of photovoltaic panels. This research presents a method to alleviate the heat problem by coating the upper surface of the photovoltaic panels with one, two, and three layers of Indium Tin Oxide nano-coating. Four cases have been tested, including a bare case and three coated models. The investigations have been carried out experimentally and numerically using ANSYS Fluent 2022 R1. However, the results in the current paper only compare the three layers coating with the non-coated reference module. The preparation procedure and optical evaluation of the Indium Tin Oxide nano-coating are presented. The nano-coating enhances the radiation penetration through the panel's surface, increases the reflected radiation, and absorbs part of the infrared rays, leading to a surface temperature drop. The numerical results show that three layers with a thickness of 200 μm have considerably reduced the module surface temperature. The experimental results showed a decrease in the average surface temperature of the solar panels by 7.4 ℃, and the improvement in output energy reached 41%.

1. INTRODUCTION

Photovoltaic conversion has been recognized as one of the most promising renewable energy technologies to eliminate environmental problems such as carbon emissions and global warming. The electrical conversion process in the solar cells can generate clean electricity directly from sunlight. Sunlight is made up of photons, which carry various amounts of energy proportional to the spectrum of wavelengths of light. Some materials, such as semiconductors, can absorb a limited energy range of photons when they are exposed to light. In contrast, other photons may pass through the material or be reflected without being absorbed. The best wavelength range for photoelectric conversion in solar cells is between 0.3 and 1.1 μm [1]. Absorption of wavelengths outside this range causes a rise in the temperature of the photovoltaic cell, which leads to reduced conversion efficiency [2]. This is due to the fact that the large drop in open circuit voltage, *Voc*, more than compensates for the marginal rise in short circuit current, *Isc* [3]. Operating temperatures can sometimes reach values above 325 K due to the absorption of photons outside the required range, and a decrease in the relative efficiency of about 0.45% can be expected for a solar cell built of crystalline silicon for every 1.0 ℃ increase in temperature [4].

The main function of radiation cooling is to enhance the heat emission of solar cells by adding a transparent cooler over the solar cells in order to increase the heat emission of solar cells while maintaining the efficiency of solar energy absorption [5]. The transparent coolant should have a high transmittance in the wavelength range associated with solar radiation and a large heat emission in the wavelength range associated with central infrared radiation [6]. It is possible to cool solar panels by reflecting their heat to a cooler outer space through a transparent window for electromagnetic waves extending between 8 and 13 μm [7], which corresponds to the peak wavelengths of heat radiation [8]. Radiative cooling attracts efforts to improve energy efficiency because it is completely passive and does not require any power input [9].

Another technology for PV radiative cooling is to manage the solar spectrum through selective spectral cooling, whereby useless photons are blocked, and allow photons that are useful in the process of converting light into electricity [10]. The literature is evident that radiative cooling is a successful technique to mitigate the accumulated heat in the PV modules. Selective coating could be adopted to achieve radiative cooling. However, the approach is state-of-the-art, and many types of selective coating for radiative cooling have not been investigated yet. More experimental work is required to optimize the coating materials and also to assess the effect of nanoadditives on the selective coating. Zhu et al. [11] designed a transparent cooler consisting of a two-dimensional square network of silica pyramids and a uniform silica layer with a

thickness of 100 µm. This coolant is optically transparent and emits as a blackbody in the mid-infrared wavelength range. The results of performance predictions showed that even at a solar heating power of 800 W/m^2, the temperature reduction of silicon solar cells with this hierarchical cooler design can reach 17.6 ℃, which subsequently leads to an improvement in the relative electrical efficiency of 7.9%.

Zhao et al. [12] developed a two-dimensional photo cooler to cool solar cells by integrating photovoltaic, thermal, and electrical simulations. It has been shown that the temperature of the solar cells may decrease by about 8 ℃. When compared to the normal PV module, implementing a complete photonic method decreases the inefficient absorption of solar light by the selected panel. At the same time, it can selectively reflect the radiation. Solar energy actively radiates heat to outer space while maintaining solar energy transmission in the photoelectric conversion range of 0.3 to 1.0 µm.

PV passive cooling could improve the electricity production performance and save the PV modules from thermal cracking. Many techniques have been attempted, and radiative cooling represents the state of the art of PV cooling. But investigation on radiative cooling by nano-coating is minimal, and not many nano-coatings have been reported. Accordingly, the objective of the current research is to investigate the effectiveness of radiative cooling by nano-coating. The investigations have been performed experimentally and computationally. Three different PV modules have been coated with Indium Tin Oxide (ITO) with different thicknesses, and one bare case is used as a reference. However, the results presented in this work focus on the coating process and preparation of the experimental models, and compare a three-layer coating with the bare PV modules.

2. RESEARCH METHODOLOGY

Figure 1 displays the working principle of the thin optical nano-coating (TONC) of solar PV. The technique is adopted in the current investigation to evaluate the coating effect on the PV performance. The upper surface, i.e., the glass cover of the PV panel, is coated for the purpose of managing the solar spectrum.

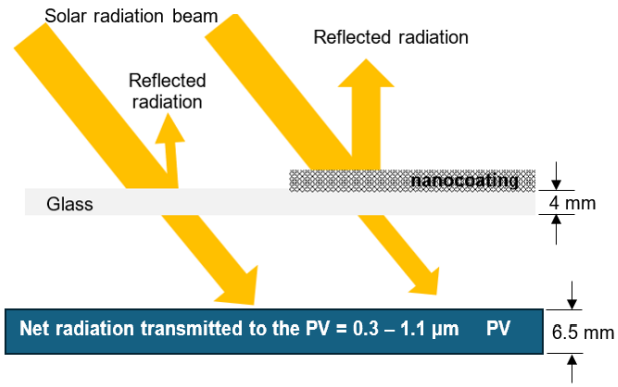

Figure 1. The working principle of the nano-coating

2.1 Experimental methodology

This section deals with the practical application of preparing a nano-coating of ITO, then spraying it on glass substrates and the glass cover of the PV panels. After the samples and the coated PV were ready, measurements were performed of the optical properties, temperature, current, voltage, and efficiency of the PV. The measurement data have been used to determine and evaluate the effect of the nanofilm. Figure 2 is a flowchart showing the steps that have been performed in the experimental methodology.

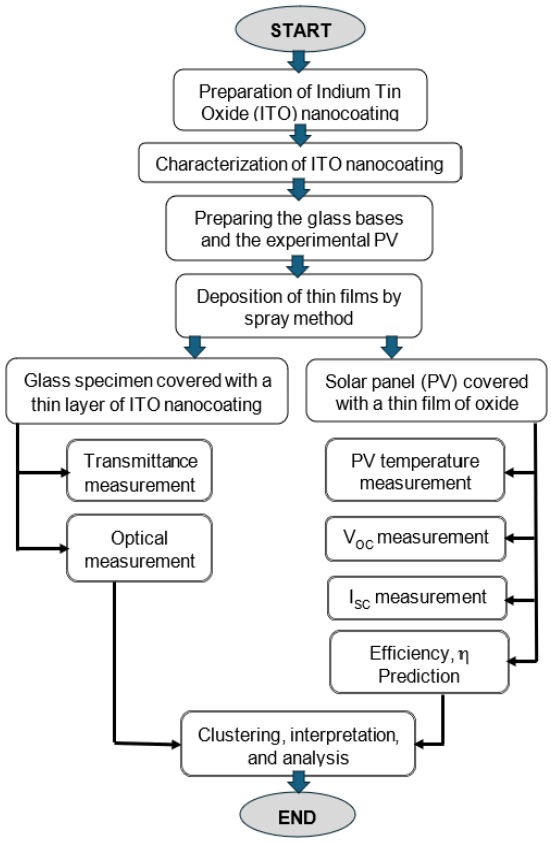

Figure 2. Flowchart of the research experimental methodology

Three polycrystalline FRS-50W PV panels were used for the experimental investigations. The power of each panel is 50 watts, and the dimensions of one panel are 500 × 670 × 35 mm. The specifications of the panels are listed in Table 1.

Table 1. Specification of the photovoltaic panel type polycrystalline at standard test conditions (AM1.5, 25 ℃, 1000 W/m^2)

Module Type	FRS-50 W
Peak Power (P_{Max})	50 W
Maximum Power Voltage (V_{MP})	18 V
Maximum Power Current (I_{MP})	2.78 A
Short Circuit Current (I_{sc})	3.17 A
Open Voltage (V_{oc})	22.05 V
Module efficiency	15%
Fill factor	75.39
Tolerance	±3%
Application Class	A
Fuse Rating	15 A
Dimensions	50 × 67 × 3.5 cm
Thermal coefficient of power	0.45%/℃
Thermal coefficient of voltage	0.34%/℃
Thermal coefficient of current	0.05%/℃

2.1.1 Preparation of Indium Tin Oxide nano-coating

ITO is a transparent conductive material commonly used in applications such as transparent electrodes in electronic

devices and solar cells. ITO nano-gels could be synthesized using the sol-gel method, which involves hydrolysis and condensation of precursor compounds containing indium and tin ions. The resulting gel can then be converted into nanoparticles or thin films, depending on the application. The following procedure has been followed to produce the nano-gel.

•Preliminary, a certain amount of 6 ml of indium chloride (InCl3) is dissolved in 50 mL of ethanol (C2H5OH). The solution should be well stirred for 15 min to ensure homogeneity. 1.5 mL of tin chloride (SnCl4) was dissolved in 55 mL of ethanol C2H5OH. The solution was left in a closed glass container and stirred totally by using magnetic stirring at 100 rpm for 2 hours at room temperature. Furthermore, the resultant mixture should be exposed to ultrasonification for 45 min for well-dispersed purposes.

•In a separate container, a small amount of acid or base catalyst was added to each precursor solution. This process initiates the hydrolysis and condensation reactions. The indium and tin precursor solutions underwent hydrolysis to form metal hydroxide species.

•A solution of a selected polymeric or organic gel matrix using polyvinyl alcohol (PVA) in a solvent was prepared as the matrix for dispersing the ITO nanoparticles. The ITO solution was mixed with the gel matrix precursor, and then the mixture was allowed to gel by letting it stand at room temperature or by gentle heating. The gel would lead to the formation of a nano-gel.

•Finally, the product solution was left for almost 2 days at room temperature.

The required devices for ITO production are shown in Figure 3(a), and detailed specifications of each device are presented in Table 2. The elemental compounds to form the nanoparticles dispersed in a gel matrix are shown in Figure 3(b), and the sources are provided in Table 2. The characterization results of the chemicals used in the research are provided in Table 3.

Table 2. The instruments used in the synthesis of Indium Tin Oxide nano-gel

The Instruments	Manufacturer
Hot plate and magnetic stirrer	Faithful SH-3
pH meter	HQ-0091
Ultrasonic bath (3 L)	JPS-20 A Vevor
Electrical Oven	Memmert, UNE 400, TEMP.250 °C
Measuring cylinder	BOMEX Chemical

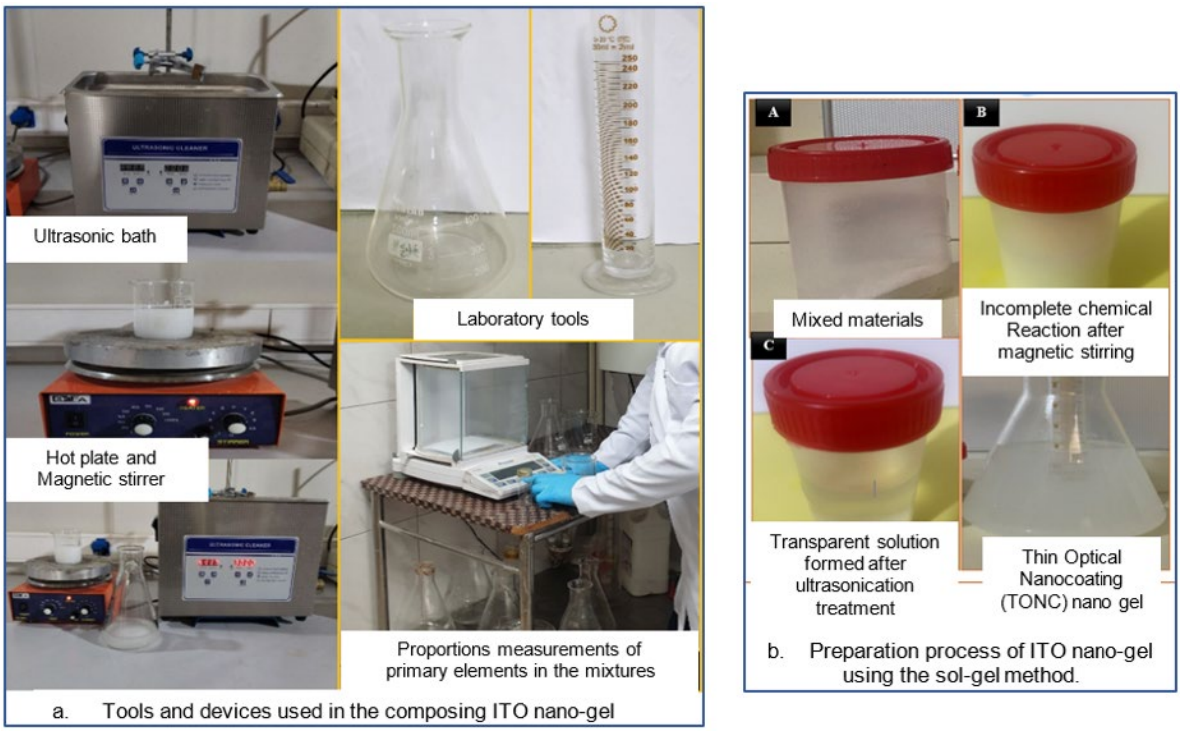

Figure 3. IOT nano-gel production: (a) Devices and instruments, (b) Process

Table 3. The chemical materials used in the preparation of Indium Tin Oxide nano gel and their characterized properties

The Chemicals	Manufacturer	Properties
Indium chloride (InCl3)	GLENTHAM (UK)	Colourless to white, soluble powder, purity 99%, surface area 200–300 m^2/g, particle size 50–60 nm
Tin chloride (SnCl4)	Sigma (USA)	Appearance is transparent or white, particle size 30–40, boiling point 114.1 °C. Density: Its density is about 3.46 grams/cm^3, purity 98%
Ethanol Absolute C2H5OH	Honeywell (Germany)	Appearance: Transparent, colourless liquid, characteristic alcoholic odour, molecular weight: 46.07 g/mol, density: about 0.789 g/cm^3 at 20 °C, melting point: -114.1 °C. Purity 99.98%
Polyvinyl alcohol (PVA)	CDH (INDIA)	
Deionized water	Al Rafidain factory (Iraq)	

2.1.2 The coating apparatus

The spray method was utilized for coating the glass substrate samples and PV panels. The coating system was composed of three parts: A spray gun and a flexible platform. The nozzle of the spray gun does not exceed Ø = 2.2 mm. The spray gun was arranged with a simple platform to ensure that the glass substrate and PV panel were fixed during the coating process. Also, to keep the exact distances between the spray gun nozzle and the coated samples, either glass substrates or solar panels, as observed in Table 4. The frame of the platform was made of wood with a metallic slide to control the spraying distance. The final arrangement was named the flexible coating platform, as shown in Figure 4.

Table 4. The experimental conditions of the coating system (spray stage)

Property	The Value or Condition
Diameter of spray gun nozzle	kept fixed at 2 mm
Separation distance between the gun nozzle and the samples	400 mm
The flow rate of coating	0.25 L/min
Capacity of spray gun tank	0.5 L
Temperature	At room temperature

Figure 4. Coating platform

2.1.3 Preamble of the glass substrates

The main purpose of using and coating glass substrates is to verify the identity of the prepared material, structure, composition, purity, thickness, morphology, and optical. Basically, these measurements cannot be achieved when using TONC on the surface of the photovoltaic panel. The glass bases used in our study were made of glass with dimensions 7.5 × 2.5 cm^2 and a thickness ranging between 3–4 mm. It is well-cleaned to remove plankton before the sedimentation process, as in the following procedure:

i. Wash the glass bases with running water to get rid of plankton resulting from environmental conditions.

ii. Rinse the glass bases with distilled water, then place them in the ultrasound machine for 10 minutes.

iii. Lift the glass bases with special tweezers and place them in a glass beaker containing 99.9% pure ethanol to remove traces of grease, if present on those bases.

iv. Finally, the substrate was dried at 110 °C in an electric oven to be ready to coat it using the spray method.

After preparing the glass samples, the coating is done using the amount of ITO gel that was prepared previously and mixed with ethanol. The dilution ratio was 5 mL of ITO nano-gel with 50 mL of ethanol. The coating solution was mixed using a magnetic stirrer for 30 min.

Next, a 60-minute ultrasonic treatment was used to ensure homogeneity of the materials at room temperature, after which the glass substrates were spray-coated, as shown in Figure 5.

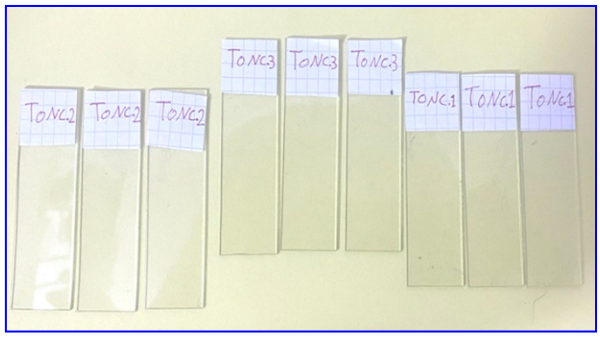

Figure 5. Models of some painted glass substrates

2.1.4 Characterize the ITO nanoparticles or gel

The characteristics and structure analysis of ITO nanoparticles or gels have been measured using state-of-the-art nano-characterization equipment as follows:

a. Transmittance analysis for the ITO gel's

Spectroscopic measurement of transmittance and absorbance, which is an optical measurement technique, is used to confirm the degree of transparency of the ITO gel and the extent of its ability to cross and reflect the manufactured light spectra to evaluate the performance of TONC on photovoltaic panels later. The Shimadzu UV-1800 is a spectrophotometer, shown in Figure 6, and is capable of measuring transmission and absorption of wavelengths with a maximum of 1100 nm and a minimum spectral bandwidth of 1.0. The device has a wavelength accuracy of 0.1 nm and a wavelength reproducibility of 0.1 nm.

Transmittance measurement was performed over the wavelength range of 300–1100 nm. The spectrophotometer is turned on at least 30 minutes before each measurement session. The calibration process has been completed before starting. The instrument features two holes, with the first hole used to measure permeability by placing a sample on it. The second slot is used to place the reference sample for comparison and then record the data.

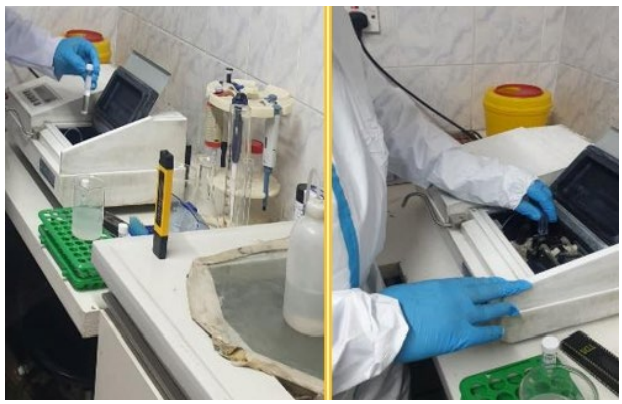

Figure 6. Measurement of optical properties of TONC using a Shimadzu UV-1800 spectrophotometer

b. Thickness measurement of thin films

Thickness measurement is one of the important and

necessary criteria for thin films, as there are several ways to measure the thickness of thin films. An FT-650 film thickness probe was used to measure the thickness of prepared films located at the Ministry of Science and Technology/Solar Energy Research Center/Renewable Energy Research Department. The FT-650 Prometrix Film Thickness (FT) Probe System provides automated measurement and mapping of your wafer. The FT tester can measure single and multiple layers of oxide, nitride, photoresist, polysilicon, SOG, and other transparent films. The probe has a measuring range of 0–3000 μm with a typical accuracy of ±1%. The measured thickness of the prepared film was 200 ± 25 nm.

c. Optical measurements

The study of transmittance and absorption spectroscopy is a very important tool for material mapping, providing useful information about the energy gap. The spectra of transmittance, absorbance, and reflectivity were measured using a spectrophotometer (optical transmittance meter, shown in Figure 7) for the wavelength range from 200 to 2500 nm. This spectrometer includes a wide part of the electromagnetic spectrum. The working principle of this device is to place the model to measure its optical properties in the designated slot and then directly display the percentages of transmittance of the transient wave spectra, through which the optical parameters are calculated.

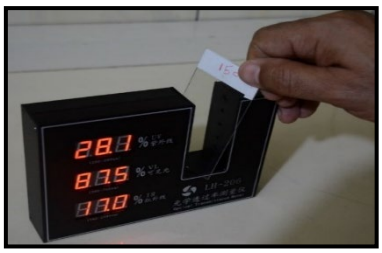

Figure 7. Optical transmittance meter to measure nanofilm-coated glass bases

2.1.5 Nnano-coating of the PV panels

After completing the process of preparing the nano layer and conducting tests on the coated glass substrates and obtaining the best results, the photovoltaic panels are now coated using spray technology. Figure 8 shows the spraying method. The spraying process was repeated several times to obtain satisfactory results. In each process, the distance between the spray nozzle and the coated samples is changed, whether they are glass substrates or solar panels, in addition to enlarging or reducing the spray nozzle and other available settings.

Figure 8. The PV panel during the coating process by the air spray method

2.1.6 Experimental setup

Practical experiments were carried out for optimal cases under the local weather conditions of the city of Baghdad, Iraq (latitude 33 degrees and longitude 44 degrees). Two panels were installed on an iron structure, one of them coated with three layers of nano-coating and the second without coating, as shown in Figure 9, which was considered a reference cell. A solar energy measuring device was used to measure the intensity of solar radiation, and it was installed vertically on the photovoltaic panels to obtain the values of incident solar radiation.

Two separate devices, AVO meters, were used to measure the current and voltage values of each solar panel to ensure quick recording of readings and reduce the percentage of error. The devices used have been pre-calibrated. The duration of the experimental study was during July and August, and August 15 was relied upon for clear weather conditions for accurate comparison. Readings were taken from 8:00 a.m. to 6:00 p.m., and all parameters, namely solar radiation intensity, *Isc, Voc, Iload, Vload*, and temperature of photovoltaic panels, were recorded for three solar systems at the same time. After some time, the experimental study ended, and a comparison was reached between the factors mentioned above.

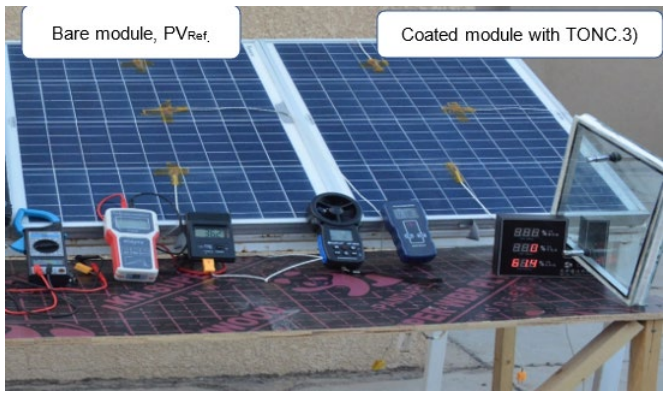

Figure 9. Experimental setup with reference and coated PV modules

2.2 Computational methodology

2.2.1 Model description

Table 5 and Table 6 show the general characteristics of the approved model and the materials used. Other material properties are set as default values in the FLUENT database material list.

2.2.2 Development of computational models

In the engineering model, the upper surface glass of the original model was coated with a nano-coating of 1, 2, or 3 layers, as shown in Figure 10. During the simulation procedure, the thickness of the nano-coating was added to the thickness of the upper glass, and they were considered one layer with similar properties to ensure the accuracy of the numerical analysis.

After one finishes drawing the models, the important volumes and walls required are selected, while the other wall that is not selected by default will be named. Each region must also be defined as either a gas or a solid. The glass panels are presented as solids, and the gas and air volume between them is presented as a gas. In the case of using nano-coating, it is considered part of the upper outer layer of the solar panel, as it is a very thin material.

Table 5. Photovoltaic properties [13-15]

Material	Property							
	Thickness (mm)	Density ρ (kg/m^3)	Thermal conductivity k (W/m·K)	Specific heat C_p (J/kg·K)	Absorptivity λ	Reflectivity σ	Transmissivity τ	Emissivity ε
Glass	3.0	1730	0.24	500	0.04	0.04	0.92	0.9
EVA	0.5	945	0.35	2070	0.08	0.02	0.9	-
Cell	0.3	2330	148	677	0.9	0.08	0.02	-
Tedlar	0.1	1350	0.2	1250	0.13	0.86	0.012	0.9
AL	2	2719	202.4	871	-	-	-	-

Table 6. Operational conditions for the current study

Item	Value or Description
Materials	PV modules: Nano-thin optical coatings unit
Dimensions of each PV module	L = 670 mm, W = 500 mm, H = 35 mm
Nano-thin optical coating module.	Nano-thin optical coating unit with Multiple layers.
Variations	Three different layers of TONC, TONC.1, TONC.2, and TONC.3
Ambient conditions	Summer, Max. Temp. 35–49 °C, Max radiation 1190 W/m^2
Inlet BC	Pressure inlet (0 pa), temperature (varying with time)
Outlet BC	Pressure outlet (0 pa)
Heat flux	Solar radiation varies with time
Location	On the terrace floor of a typical building in Baghdad

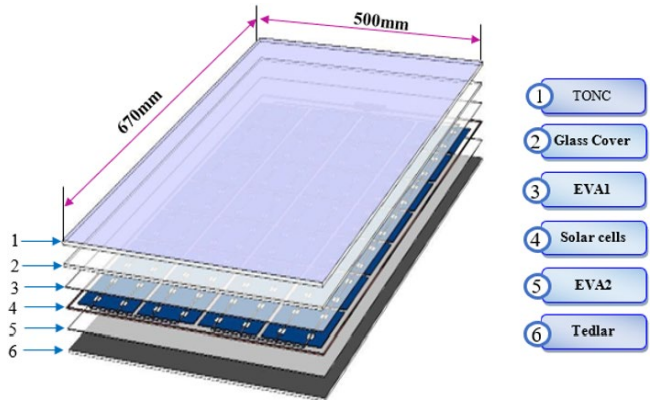

Figure 10. Geometrical model of thin optical nano-coating TONC model

2.2.3 Assumptions and mathematical modelling

Choosing the related ambient conditions is important for an accurate evaluation of cooling contribution. In fact, there is a reduction in the temperature due to radiative cooling, which can be increased based on the boundaries of radiation, surrounding conditions, and wind characteristics. However, it is necessary to assign a point as a reference for comparison purposes. The conducive and radiative cooling are mostly required to maintain the temperature near its reference point and to maximize the power. Some main conditions are mentioned in Table 5. In addition to the boundary conditions, some assumptions are necessary for proper thermal modelling, such as:

•Three-dimensional model.

•Transient simulation.

•The gravity is 9.81 m/sec^2 downward.

•The temperature in the normal direction through the layers of the PV module is uniform throughout.

•It is presumed that their thermophysical values remain constant regardless of temperature variations.

•It is presumed that the electrical resistance losses in solar cells are insignificant.

•The heat source affecting the solar cell is solar radiation, varying with time.

a. Energy analysis

The energy balance of radiative cooling on the PV module can be analyzed as shown in Figure 11. A resultant energy term is known as P_{cool} for the radiative cooling yields [16]:

$$P_{cool}(T) = P_{rad}(T) - [P_{atm}(T_{amb}) + P_{solar} + P_{cond+conv}(T_s, T_{amb})] \quad (1)$$

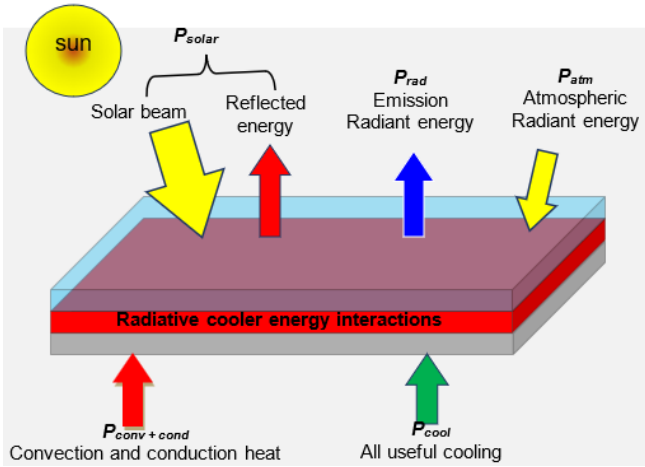

Figure 11. Energy balance of passive radiative cooling of a solar PV panel

b. Short circuit current and open circuit voltage

The short circuit current, *Isc* is obtained if the solar cell is short-circuited, i.e., there is no voltage at the cell. The open circuit voltage, *Voc*, is obtained when no current is drawn from the solar cell. The *Isc* and *Voc* can be determined by using Eqs. (2) and (3), respectively [17].

$$I_{sc} = I_{rf}(1 + \beta_{ref}(T_{sc} - T_{rf}) \quad (2)$$

$$V_{oc} = V_{rf}(1 - \beta_{ref}(T_{sc} - T_{rf}) \quad (3)$$

where, β_{ref} is a temperature coefficient, T_{sc} is the temperature of PV, and T_{ref} is the reference temperature, 25 °C.

c. Cell efficiency

The solar efficiency of a photovoltaic system is known as the ratio of the produced power to incident radiation and is expressed as follows [18]:

$$\eta_{sc} = \frac{P_{max}}{\mathrm{GA}} = \frac{I_{sc} * V_{oc}}{GA} \quad (4)$$

or

$$\eta_{sc} = \eta_{ref}(1 - \beta_{ref}(T_{sc} - T_{ref})) \quad (5)$$

where, η_{ref} is the original efficiency of the panel (η_{ref} = 0.15), and β_{ref} is a coefficient (β_{ref} = 0.0045 1/C).

2.2.4 Mesh generation

Lattice independence analysis was performed on a thin optical nano-coating with different multilayers of TONC, as shown in Figure 12.

Simulation results of solar panels with TONC at varying degrees of grid resolution are compared. It was found that the hexagonal mesh with an element size of 3 mm gave the best acceptable results with no significant decrease in accuracy. In contrast, the time required for mesh generation and analysis is reduced by approximately half compared to the case using tetrahedral cells, as the geometry is well-defined. Therefore, when the geometry is clear, it is generally recommended to use a hexahedral mesh [16]. The number of nodes reached 4,640,413, and the number of elements was 2,256,879.

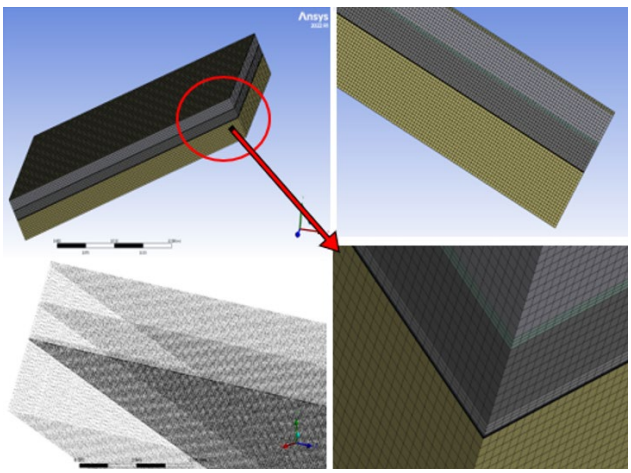

Figure 12. Tested meshes of type hexahedral cells with 3 mm element size

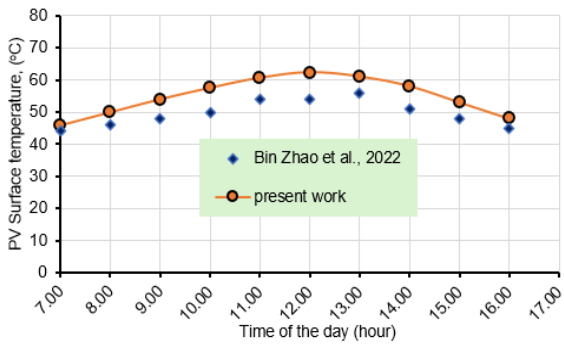

Figure 13. Numerical validation with a model from published literature

2.2.5 Validation of numerical procedure

The results of the thermal behaviour of the solar panels were validated by comparison to the results of Zhao et al. [17]. As shown in Figure 13, the results of the current study agree satisfactorily with the experimental and numerical data published by Zhao et al. [17], where the highest percentage of error between the two studies was 12.3%, and the lowest percentage of error reached 3.2%, while the average error rate was close to 7.79%.

3. RESULTS AND DISCUSSION

3.1 Numerical results

This section discusses the numerical results of using thin nano-coating TONC with the photovoltaic model with different layers (1–3 layers). In general, it can be explained how nano-coating affects the surface temperature and efficiency of the solar panel as follows:

3.1.1 Effect of TONC on PV temperature

The simulation results of surface temperature, shown in Figure 14, prove that the use of the proposed nano-coating has a direct effect on the surface temperature of the solar panel. This is mostly due to the reflection of thermal rays that fall outside the wavelength at which the solar cell operates, which falls between 0.3–1.1 µm. Photons outside this range are responsible for the temperature increase that occurs, the greater the loss of solar radiation outside the range.

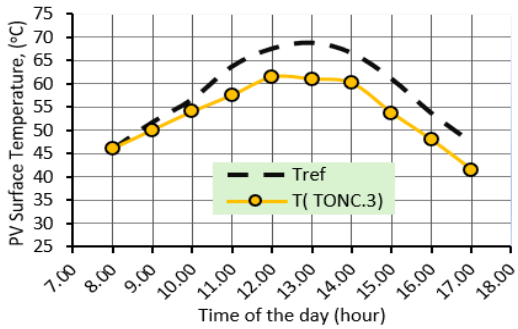

Figure 14. Variation of PV panel surface temperature over time

When the PV panel was coated with a three-TONC layer, the highest temperature of the panel surface reduction reached 7.34 °C. This can be explained by the fact that when light hits the nanolayer, it is scattered and reflected several times, especially at long wavelengths. This multiple scattering increases the path of light within the nanolayer and thus increases the probability of absorbing the thermal energy carried by the rays.

In addition, these nano-coatings reflect or absorb infrared rays responsible for heat transfer and convert them into other energy, such as molecular motion, reducing heat transfer through the glass. By using nano-coating, the thermal insulation efficiency of the glass can be improved, thus reducing heat transfer through it. From the above, we note that the ideal number of layers to reduce temperature is three layers, which prompted us to test it experimentally. From the above, we note that the ideal number of layers to reduce temperature is three layers, which prompted us to test it experimentally.

3.1.2 Effect of TONC.3 on the PV efficiency

The solar panel coated with nanofilm showed higher efficiency than the panel without nanofilm coating. This seems logical as a result of the decrease in the cell surface temperature, which had a positive impact on the conversion efficiency in peak hours after midday to 13.5%. When the solar panel was coated with three layers of nano-coating, without the nano-coating, the PV system showed an efficiency of 12.3% for the same operating conditions, as shown in Figure 15.

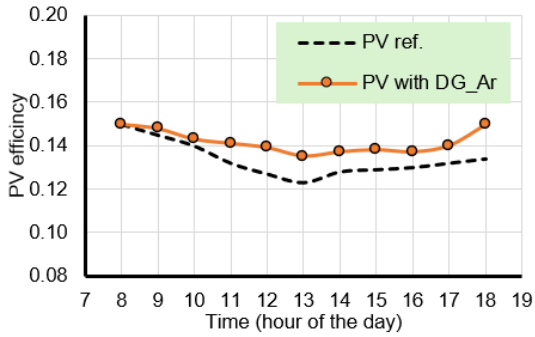

Figure 15. Variation of efficiency over time for a photovoltaic cell with and without TONC.3

3.1.3 Temperature distribution

Figure 16 shows the temperature distribution in the numerical test on the cell surface for the optimal case when using the three-layer coating, TONC.3. In general, the surface temperature of the panel decreased throughout daylight hours when using the TONC.3. Nano coating compared to the reference panel, and the temperature decreased clearly to reach 61.46 ℃ at the peak hour, which is 1:00 p.m., as these layers worked to reflect thermal rays with wavelengths higher than (1.1 µm). It is part of the infrared radiation that causes the surface temperature of the photovoltaic panel to rise.

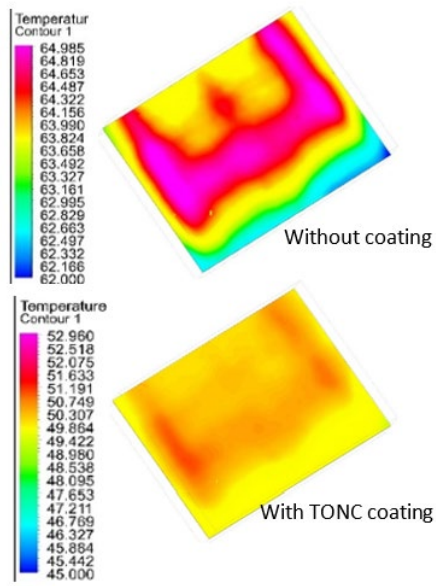

Figure 16. The temperature distribution over the PV panel with and without TONC.3

3.2 Experimental results

In this section, the experimental results of using nanophotonic coatings with a photovoltaic panel and the extent of their impact on the temperature of the solar panel and the rest of the main parameters of solar cells, such as current, voltage, and power, as well as the overall efficiency of the solar panel, will be presented.

3.2.1 Surface temperature of PV panel

Figure 17 shows the gradual change in temperature of the solar panel due to the thermal insulation provided by the TONC.3. The nanolayer helped increase the emission of unwanted rays outside the solar panel. In addition, the process of repeating the nanolayer helped reflect and absorb infrared rays at a wavelength higher than 1.1 µm due to its optical properties. It led to a decrease in the surface temperature of the solar panel. The maximum improvement in the temperature of the solar panel was at one o'clock in the afternoon when it reached 7.2 ℃, which reflected positively on the efficiency of the electrical conversion of the solar panel, which will be discussed later.

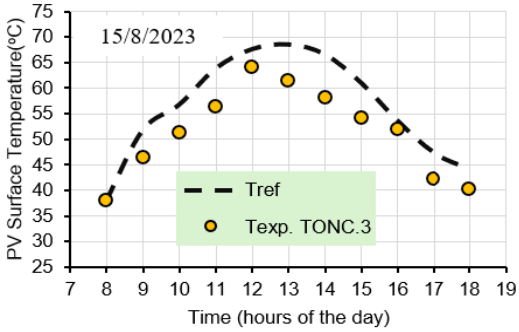

Figure 17. Surface temperature of the PV panel without and with the TONC.3

3.2.2 Short circuit current

Figure 18 shows the variation of short-circuit current for PV panels with and without nano-coating with time on July 15, at peak solar radiation at 1:00 p.m. It is observed that the current of the coated plate is slightly higher than that of the plate without coating in all cases. The short-circuit current depends on solar radiation and the ambient temperature. The increase in short circuit current with increasing ambient temperature is very small but linearly related to the solar intensity. This explains the difference in short-circuit current, which is determined by the change in solar radiation.

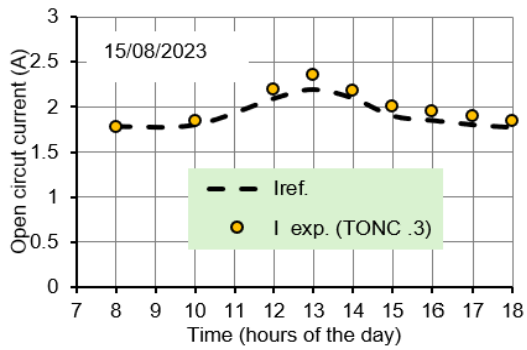

Figure 18. Hourly change in the open circuit current of a photovoltaic panel with and without a TONC.3

It is noted that the highest percentage increase in the current value reached 0.15% between the painted panel and the

reference during peak hours at 13:00. Then, after, the current value decreases in general as a result of the reduction in solar irradiation, reaching 1.85 A at 18:00 for the painted panel, and 1.77 A for the reference PV module. This slight difference between using the nano-coating and the reference plate indicates that the current is slightly affected by increasing temperatures.

3.2.3 Open-circuit voltage

The open circuit voltage of the reference and coated photovoltaic panels during daylight hours is shown in Figure 19. The open circuit voltage depends on solar radiation and the temperature of the surrounding environment. The open circuit voltage values measured for the painted panel were slightly higher than the reference panel in all cases. This is due to the decrease in the temperature of the painted panel due to the presence of paint, as we explained in the section on the effect of paint on the surface temperature of the panel. Over time, heat leads to a decrease in the open circuit voltage, and this appears more evident when comparing the increase with the increase in solar radiation. The highest open circuit voltage values for the reference board were 21.4 volts compared to 20.5 volts for the coated board at 13:00. It can be seen that the photovoltaic voltage is inversely proportional to solar radiation and ambient temperature.

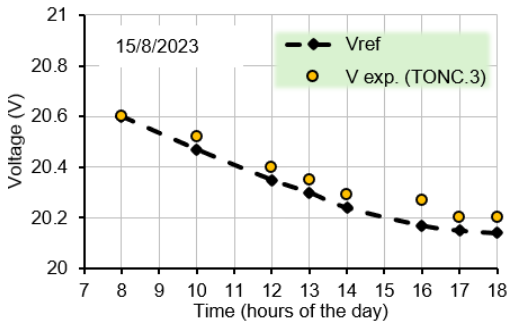

Figure 19. Hourly change in the open circuit voltage of a photovoltaic panel with and without TONC.3

3.2.4 Power

Figure 20 displays the measured values of the output power for the three-layer nano-coated panels by TONC.3 and the reference panel. The average improvement in the power is 7.3%. The maximum difference in the average output power developed by the PV panel was recorded as 3.4 W. This power improvement is due to the nano-coating effect, which improves the impermeability of infrared radiation as well as heat dissipation to the surrounding areas by natural convection.

3.2.6 Electrical efficiency

Figure 21 shows the variation of the electrical efficiency of the two three-layer nano-coated panels (TONC.3) and the reference photovoltaic panel, with daylight hours on the test day on July 15. The average electrical efficiency difference between the two panels was 0.8%. The electrical efficiency of photovoltaic panels decreases as solar radiation increases. When solar radiation increases, the electrical efficiency of reference photovoltaic panels decreases from 15.1% to 11.3%. It could be concluded that the operating temperature of the cell increases when the solar energy density value is high. Hence, the electrical efficiency decreased. However, for the painted panel (TONC.3), part of the electrical efficiency was recovered by radiative cooling.

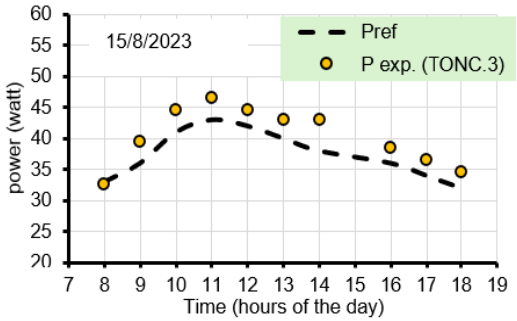

Figure 20. Variation of the PV power with and without nano-coating (TONC.3)

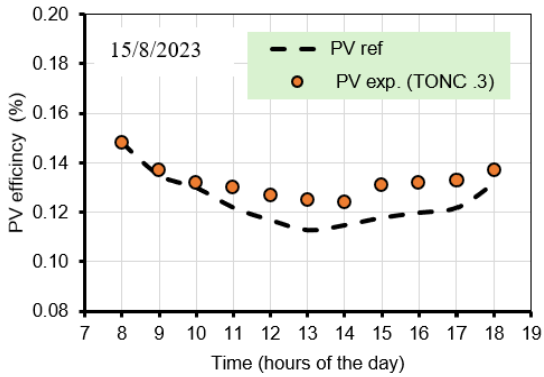

Figure 21. Variation of the PV efficiency with and without nano-coating (TONC.3)

3.3 Comparison between numerical and experimental results

To prove the accuracy of the numerical results, geometric and parametric conditions exactly similar to those of the experimental instrument were used. Therefore, the ambient air and operating air temperatures were measured for ten hours, and the operating hours were compared. According to these numbers, it is clear that there is a satisfactory convergence between the results obtained from the CFD solution and the results obtained from the experimental work, as the maximum variation in the surface temperature of the photovoltaic panel between the numerical and experimental results reached 7.6%, as shown in Figure 22.

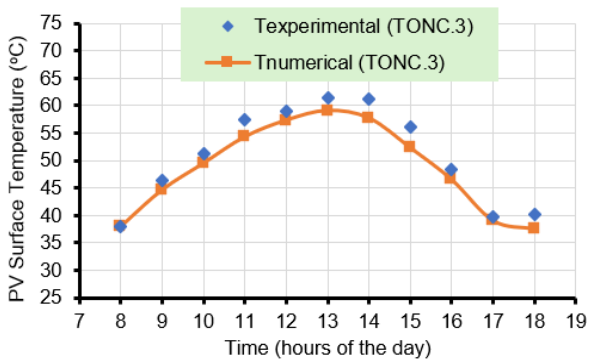

Figure 22. Comparison between numerical and experimental results for temperatures

The reasons for this discrepancy are due to the measuring

devices used, as well as the theories that were assumed in the numerical solution, and the accuracy of some of the material properties that were determined. ANSYS software accessed.

4. CONCLUSIONS

In the current research, the outer glass coating of solar panels is coated with multilayer nanolayers of ITO (one, two, or three layers) to prevent unwanted rays from reaching the solar panels. Experimental results for both the conventional and improved models also validated the numerical results. Below is a summary of the most important conclusions obtained from the analysis of each effect within the framework of the current study.

•The average drop in surface temperature of the panel was 7.4 ℃ when coated with nano-coating in three layers.

•The improvement in energy output reached 41%.

•The improvement in maximum efficiency reached 13.8% for the nano-coated panel compared to 11.3% for the reference panel under the same operating conditions.

It is recommended to investigate the extra-thin nanofilms to boost the spectral emissivity on the surface of solar cells in order to cool them.

ACKNOWLEDGMENT

The author would like to thank Mustansiriyah University - Baghdad - Iraq for the technical support to perform the experimental research of the work.

REFERENCES

[1] Zhao, B., Hu, M., Ao, X., Xuan, Q., Pei, G. (2020). Spectrally selective approaches for passive cooling of solar cells: A review. Applied Energy, 262: 114548. https://doi.org/10.1016/j.apenergy.2020.114548

[2] Al-Kayiem, H.H., Reda, M.N. (2021). Analysis of solar photovoltaic panel integrated with ground heat exchanger for thermal management. International Journal of Energy Production and Management, 6(1): 17-31. https://doi.org/10.2495/eq-v6-n1-17-31

[3] Dubey, S., Sarvaiya, J.N., Seshadri, B. (2013). Temperature dependent photovoltaic (PV) efficiency and its effect on PV production in the world—A review. Energy Procedia, 33: 311-321. https://doi.org/10.1016/j.egypro.2013.05.072

[4] Perrakis, G., Tasolamprou, A.C., Kenanakis, G., Economou, E.N., Tzortzakis, S., Kafesaki, M. (2020). Passive radiative cooling and other photonic approaches for the temperature control of photovoltaics: A comparative study for crystalline silicon-based architectures. Optics Express, 28(13): 18548. https://doi.org/10.1364/oe.388208

[5] Mandal, J., Fu, Y., Overvig, A.C., Jia, M., Sun, K., Shi, N.N., Zhou, H., Xiao, X., Yu, N., Yang, Y. (2018). Hierarchically porous polymer coatings for highly efficient passive daytime radiative cooling. Science, 362(6412): 315-319. https://doi.org/10.1126/science.aat9513

[6] Li, Z., Ahmed, S., Ma, T. (2021). Investigating the effect of radiative cooling on the operating temperature of photovoltaic modules. Solar RRL, 5(4): 2000735. https://doi.org/10.1002/solr.202000735

[7] Rephaeli, E., Raman, A., Fan, S. (2013). Ultrabroadband photonic structures to achieve high-performance daytime radiative cooling. Nano Letters, 13(4): 1457-1461. https://doi.org/10.1021/nl4004283

[8] Wang, Z., Kortge, D., Zhu, J., Zhou, Z., Torsina, H., Lee, C., Bermel, P. (2020). Lightweight, passive radiative cooling to enhance concentrating photovoltaics. Joule, 4(12): 2702-2717. https://doi.org/10.1016/j.joule.2020.10.004

[9] Ghadikolaei, S.S.C. (2021). Solar photovoltaic cells performance improvement by cooling technology: An overall review. International Journal of Hydrogen Energy, 46(18): 10939-10972. https://doi.org/10.1016/j.ijhydene.2020.12.164

[10] Mojiri, A., Taylor, R., Thomsen, E., Rosengarten, G. (2013). Spectral beam splitting for efficient conversion of solar energy—A review. Renewable and Sustainable Energy Reviews, 28: 654-663. https://doi.org/10.1016/j.rser.2013.08.026

[11] Zhu, L., Raman, A., Wang, K.X., Anoma, M.A., Fan, S. (2015). Radiative cooling for solar cells. In Physics, Simulation, and Photonic Engineering of Photovoltaic Devices IV - San Francisco, United States, p. 935814. https://doi.org/10.1117/12.2080148

[12] Zhao, B., Hu, M., Ao, X., Xuan, Q., Pei, G. (2018). Comprehensive photonic approach for diurnal photovoltaic and nocturnal radiative cooling. Solar Energy Materials and Solar Cells, 178: 266-272. https://doi.org/10.1016/j.solmat.2018.01.023

[13] Bijarniya, J.P., Sarkar, J., Maiti, P. (2020). Review on passive daytime radiative cooling: Fundamentals, recent researches, challenges and opportunities. Renewable and Sustainable Energy Reviews, 133: 110263. https://doi.org/10.1016/j.rser.2020.110263

[14] Yazdanifard, F., Ameri, M., Ebrahimnia-Bajestan, E. (2017). Performance of nanofluid-based photovoltaic/thermal systems: A review. Renewable and Sustainable Energy Reviews, 76: 323-352. https://doi.org/10.1016/j.rser.2017.03.025

[15] Shen, C., Zhang, Y., Zhang, C., Pu, J., Wei, S., Dong, Y. (2021). A numerical investigation on optimization of PV/T systems with the field synergy theory. Applied Thermal Engineering, 185: 116381. https://doi.org/10.1016/j.applthermaleng.2020.116381

[16] Tadepalli, S.C., Erdemir, A., Cavanagh, P.R. (2011). Comparison of hexahedral and tetrahedral elements in finite element analysis of the foot and footwear. Journal of Biomechanics, 44(12): 2337-2343. https://doi.org/10.1016/j.jbiomech.2011.05.006

[17] Zhao, B., Lu, K., Hu, M., Liu, J., Wu, L., Xu, C., Xuan, Q., Pei, G. (2022). Radiative cooling of solar cells with micro-grating photonic cooler. Renewable Energy, 191: 662-668. https://doi.org/10.1016/j.renene.2022.04.063

[18] Ahmed, S., Li, Z., Javed, M.S., Ma, T. (2021). A review on the integration of radiative cooling and solar energy harvesting. Materialstoday Energy, 21: 100776. https://doi.org/10.1016/j.mtener.2021.100776

NOMENCLATURE

A	the surface area of the solar cell, m^2

G	solar irradiance, W/m^2
T_{ref}	reference temperature, 25℃
T_{sc}	solar cell operating temperature, ℃
I_{sc}	short circuit current, A
V_{oc}	open voltage, v
η_{ref}	the efficiency of the solar cell at 25℃
η_{sc}	efficiency of solar cell
β_{ref}	temperature coefficient
TONC	Thin Optical Nano Coating
TONC.1, 2, 3	one, two, or three layers of thin optical nano-coating